Numerical simulations of the impact of wavefront phase distortions of pump on the beam quality of OPA

Fuling Zhang (张福领)[1*], Yanhai Wang (王艳海)[1,2], Meizhi Sun (孙美智)[1], Qunyu Bi (毕群玉)[1], Xinglong Xie (谢兴龙)[1], and Zunqi Lin (林尊琪)[1]

[1] *National Laboratory of High Power Laser Physics, Shanghai Institute of Optics and Fine Mechanics, Chinese Academy of Sciences, Shanghai 201800, China*

[2] *College of Sciences, Hebei University of Science and Technology, Shijiazhuang 050018, China*

[*] *E-mail: flzhang666@163.com*

Received April 16, 2009

A numerical model of optical parametric amplification (OPA) is introduced to investigate the impact of wavefront phase distortion of pump on the beam quality of signal. Numerical results show that the unidentical walk-off directions of the pump and the idler waves are the main factors leading to the transfer of wavefront phase distortions of the pump to the signal, and by reducing the angle between the two directions, the beam quality factor (M^2) can be greatly decreased and hence the good beam quality of the signal can be maintained.

OCIS codes: 190.4410, 190.4970, 140.4480.
doi: 10.3788/COL20100802.0217.

Optical parametric chirped pulse amplification (OPCPA) is a new technique that combines optical parametric amplification (OPA) with chirped pulse amplification (CPA), and it has become a common technique to achieve ultrashort and ultrahigh intensity laser pulses in recent years[1]. In many laser facilities, the utilization of OPCPA to amplify the stretched laser pulse has become the hot topic, and has been extensively investigated theoretically and experimentally. Most of the researches on OPA were focused on the stability, temporal pulse contrast, and parametric conversion efficiency[2−6]. However, the researches on the beam quality of OPA, such as pump-phase-to-signal-amplitude coupling, the wavefront distortions transfer among signal, idler, and pump pulses, were paid less attention to. It might not be a problem for most low-energy OPCPA systems where the pump laser sources were diffraction-limited[7]. The signal beam quality, however, will be degraded for high-energy OPCPA systems, when the wavefront phases of the pump laser sources are distorted seriously. In fact, several papers did consider the beam quality in OPCPA systems[8,9], which mainly focused on the pump-to-signal phase transfer in OPA system with collinear configuration. Their numerical simulations have shown that the transfer of phase distortions from the pump beam to the signal is due to the walk-off effect, and the walk-off-compensated crystal pair is capable of reducing the phase transfer. But in noncollinear OPA process, such as the front-end OPCPA systems of large, petawatt (PW) Nd:glass laser systems, the scheme of walk-off-compensated crystal pair to reduce the phase transfer cannot work effectively because of the noncollinear propagation of pump, idler, and signal. In this letter, we focus on the spatial beam quality of OPCPA, and thus we do not make an explicit difference between OPA and OPCPA in the following sections. We simulate a noncollinear OPA process to study the impact of spatial walk-off and the noncollinear configuration on the spatial beam quality of signal, when the wavefront phase of pump laser sources is distorted seriously. Our study is motivated by the current requirement of the OPCPA front end with high conversion efficiency, high stability, and good beam quality for SG-II PW system. Our numerical studies may be helpful for the design of the OPCPA front end.

It is important to consider the case of noncollinear geometry, which leads to the separation of the signal from the idler and the pump. The coupled-wave equations for OPA[10,11], taking into account the full spatial and temporal dependence, with type-I phase matching and nonlinear geometry configuration, can be written as

$$\begin{aligned}
&\frac{\partial E_{\rm s}}{\partial z}+\tan\rho_{\rm s}\frac{\partial E_{\rm s}}{\partial y}-\frac{1}{2{\rm j}n_{\rm s}k_{\rm s}\cos\rho_{\rm s}}\left(\frac{\partial^2}{\partial x^2}+\frac{\partial^2}{\partial y^2}\right)E_{\rm s}\\
&=-{\rm j}\frac{\omega_{\rm s}d_{\rm eff}}{cn_{\rm s}\cos\rho_{\rm s}}E_{\rm i}^{*}E_{\rm p}{\rm e}^{-{\rm j}\Delta kz},\\
&\frac{\partial E_{\rm i}}{\partial z}+\tan\rho_{\rm i}\,(t)\,\frac{\partial E_{\rm i}}{\partial y}-\frac{1}{2{\rm j}n_{\rm i}k_{\rm i}\cos\rho_{\rm i}}\left(\frac{\partial^2}{\partial x^2}+\frac{\partial^2}{\partial y^2}\right)E_{\rm i}\\
&=-{\rm j}\frac{\omega_{\rm i}d_{\rm eff}}{cn_{\rm i}\cos\rho_{\rm i}}E_{\rm s}^{*}E_{\rm p}{\rm e}^{-{\rm j}\Delta kz},\\
&\frac{\partial E_{\rm p}}{\partial z}+\tan\rho_{\rm p}\frac{\partial E_{\rm p}}{\partial y}-\frac{1}{2{\rm j}n_{\rm p}k_{\rm p}}\left(\frac{\partial^2}{\partial x^2}+\frac{\partial^2}{\partial y^2}\right)E_{\rm p}\\
&=-{\rm j}\frac{\omega_{\rm p}d_{\rm eff}}{cn_p}E_{\rm s}E_{\rm i}{\rm e}^{{\rm j}\Delta kz},
\end{aligned}\tag{1}$$

where the subscripts i, s, and p refer to the idler, signal, and pump waves, respectively. n is the linear refractive index coefficient of the crystal, $\mathbf{k}$ is the wave vector in vacuum, $\rho_{\rm s}$, $\rho_{\rm i}$ are the noncollinear angles among the wave vectors, and $\rho_{\rm p}$ is the walk-off angle of pump pulse in the y direction. The coefficient $d_{\rm eff}$ is the effective nonlinear mixing coefficient, and Δk is the crystal phase mismatch per unit length.

We can obtain the phases in a three-wave mixing process by solving the imaginary parts of Eq. (1), and the

impact of the diffraction effects on the wavefront distortion is very little and can be neglected as

$$\frac{\partial\phi_{\rm s}}{\partial z}+\tan\rho_{\rm s}\frac{\partial\phi_{\rm s}}{\partial y}=-\frac{\omega_{\rm s}d_{\rm eff}}{cn_{\rm s}\cos\rho_{\rm s}}\frac{A_{\rm i}A_{\rm p}}{A_{\rm s}}\cos\theta,$$
$$\frac{\partial\phi_{\rm i}}{\partial z}+\tan\rho_{\rm i}\frac{\partial\phi_{\rm i}}{\partial y}=-\frac{\omega_{\rm i}d_{\rm eff}}{cn_{\rm i}\cos\rho_{\rm i}}\frac{A_{\rm s}A_{\rm p}}{A_{\rm i}}\cos\theta,$$
$$\frac{\partial\phi_{\rm p}}{\partial z}+\tan\rho_{\rm p}\frac{\partial\phi_{\rm p}}{\partial y}=-\frac{\omega_{\rm p}d_{\rm eff}}{cn_{\rm p}\cos\rho_{\rm p}}\frac{A_{\rm i}A_{\rm s}}{A_{\rm p}}\cos\theta, \quad (2)$$

where $\phi_{\rm s},\phi_{\rm i},\phi_{\rm p}$ are the phases of signal, idler, and pump wave-fronts, respectively. And θ is defined by

$$\theta=\Delta kz+\phi_{\rm p}-\phi_{\rm s}-\phi_{\rm i}. \quad (3)$$

The initial phases of pump and signal waves are determined by the input waves, and if there is no input idler intensity, the initial idler phase $\phi_{\rm i}(0)$ will self-adjust to ensure the maximum initial signal gain, in which case $\phi_{\rm i}(0)=\phi_{\rm p}(0)-\phi_{\rm s}(0)-\pi/2$. If there is no walk-off effect, the spatial distribution of angle θ is uniform, the spatial phase of the amplified signal is independent of the initial phase of the pump, and it is possible to maintain the beam quality of the original signal, although we use a pump with spatial phase aberrations[3]. In the initial stage of amplification process, there exists phase distortion in the wavefronts of pump and idler, and the wavefront of initial signal can be assumed as plane. If the walk-off directions of the pump and signal are in the same side, as shown in Fig. 1(a), where $\mathbf{s}_{\rm p}$ is the Poynting vector of the pump, the wavefront phases between the pump and the idler waves will undergo spatial relative displacement, and the spatial distribution of angle θ is not uniform any more. Thus, the wavefront phase distortion of the pump will transfer to that of the signal, which results in the degradation of the beam quality of the signal. If the walk-off directions of the pump and the idler are nearly identical, as shown in Fig. 1(b), the wavefront phases between the pump and the idler waves will not undergo spatial relative displacement, and the spatial distribution of angle θ is uniform. The wavefront distortion of pump will mainly be transferred to the idler instead of the signal, and hence the good beam quality of the signal can be maintained.

An OPA system was simulated with parameters similar to those of the OPCPA front-end system of the SG-II PW upgrade facility[12,13]. In the numerical model, the seed pulse characteristics provided by a commercial mode-locked, Nd:glass laser system with a pulse width of 220 fs were used. Since the stretched pulse width is in the nanosecond regime, the effects of the group-velocity mismatch between the pump, the signal, and the idler pulses are small and can be neglected in the analysis. Moreover, group-velocity dispersion is also negligible. A split-step algorithm based on the fast Fourier transform is employed to solve the coupled-wave equations in the space-time domain, and spatial walk-off effect and noncollinear propagation were performed in the spatial-frequency domain. The pump at 532 nm has a tenth-order super-Gaussian temporal and spatial shape and an intensity of 1 GW/cm^2 with full-width at half-maximum (FWHM) of 4 ns and 2 mm. The seed at 1053 nm is Gaussian in time and space with FWHM of 3 ns and 2 mm. The seed input energy is 500 pJ. The length of the LiB_3O_5 (LBO) crystals is 60 mm. The pump walk-off angle is 0.41°.

To characterize the wavefront distortions at an instant of time, we calculate the two values of Siegman's M^2 of the output signal wave[14−16]. One, M_y^2, is calculated in the walk-off plane, and the other, M_x^2, is calculated in the plane perpendicular to walk-off. The quantities of M_x^2 and M_y^2 are defined by

$$M_x^2(t)=4\pi\sigma_{0x}(t)\sigma_{fx}(t), \quad (4)$$
$$M_y^2(t)=4\pi\sigma_{0y}(t)\sigma_{fy}(t). \quad (5)$$

They are the products of the real-space variance and the spatial-frequency-space variance of intensity for a real beam normalized to that for an ideal Gaussian beam. M^2 of 1 corresponds to a Gaussian beam with no phase distortions. Any amplitude or phase distortion makes M^2 larger than unity.

The transmitted wavefront distortion for a laser rod was about 0.5−4λ[17]. We assume the peak-to-valley (PV) value of the wavefront distortion of the initial pump is 0.6λ, as shown in Fig. 2, and the wavefront of initial

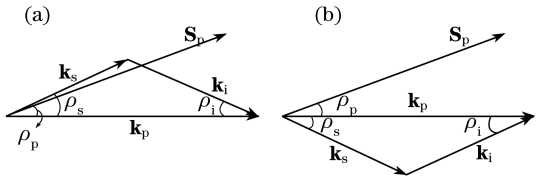

Fig. 1. Phase-matching **k**-vector triangle for noncollinear OPA.

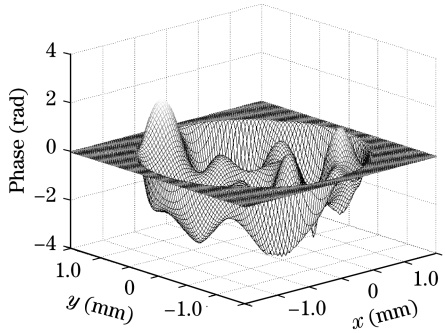

Fig. 2. Wavefront distortion of pump laser pulse.

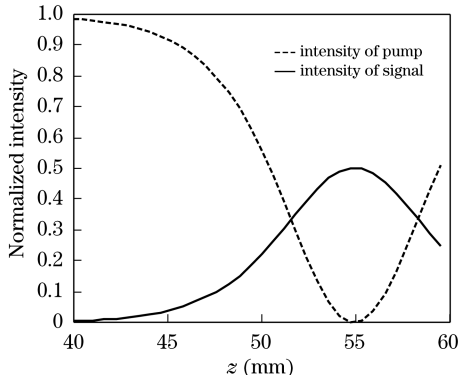

Fig. 3. Pump and signal intensity conversion versus crystal length.

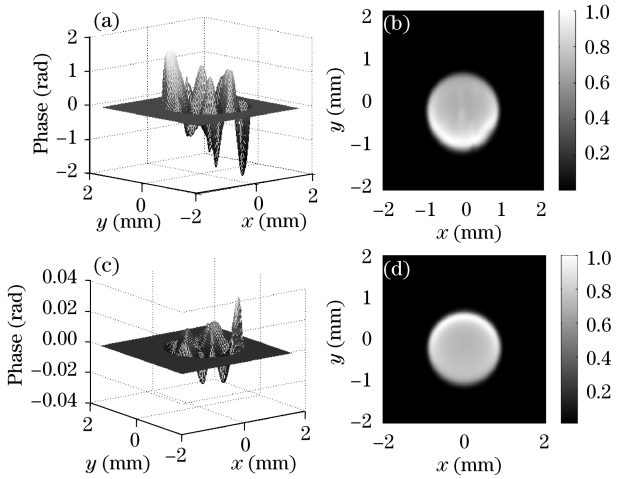

Fig. 4. (a), (c) Wavefront distribution and (b), (d) temporally integrated, normalized output beam shapes of the amplified signals, corresponding to the cases of Figs. 1(a) and (b).

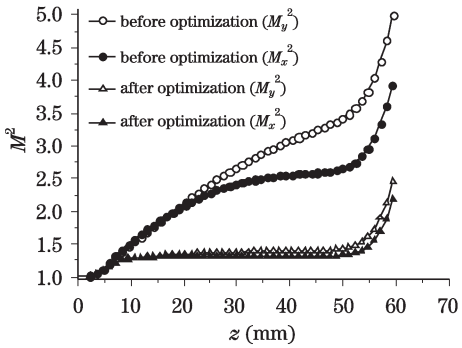

Fig. 5. M^2 at the temporal center of signal pulse versus crystal length.

signal is plane. Figure 3 plots the normalized pump and signal intensity conversion versus crystal length, and energy transferring from the pump to signal begins to reverse as the interaction length reaches 55 mm in the crystal, with the largest gain of about 10^8. Figures 4(a), (b), (c), and (d) show the wavefront distributions of the amplified signal corresponding to the cases of Figs. 1(a) and (b), respectively. Figures 1(a) and (b) show the noncollinear beam angle of 0.5° and –0.41°, respectively. For Fig. 4(a), the PV value of wavefront distortion of amplified signal is 0.59λ, which is almost equal to that of the pump (0.6λ), but the corresponding value for Fig. 4(c) is very little (0.005λ). The reason why the value of wavefront distortion in Fig. 4 can be sharply reduced is that the wavefront phases between the pump and idler waves do not undergo spatial relative displacement. So the quality of the wavefront of the signal can be maintained by tuning the noncollinear angle ρ_s appropriately to reduce the angle between the walk-off direction of pump and the direction of $\mathbf{k}_i$. Spatial variations in saturation and reconversion can produce intensity modulation and beam asymmetry in the walk-off direction. So the signal beam is asymmetry in the walk-off direction (y) but is symmetrical in the perpendicular direction (x), as shown in Figs. 4(b) and (d).

Figure 5 illustrates M^2 at the temporal center of the signal beam versus crystal length. It shows that the value of M^2 decreases greatly by reducing the angle between the walk-off direction of pump and the direction of idler. It also can be seen that the declining trend of the beam quality is gentle at the point about 53 mm, and it becomes sharp in the following interaction length. This is because, at this point, the optical parameter process runs in saturation and the intensity coupling between the interaction beams abates the declining trend, and with increasing the interaction length, the center-sunken spatial beam shapes induced by the supersaturation of OPA result in the sharp increase of M^2. Figure 5 also shows that the value of M_y^2 is larger than M_x^2 for the two cases, which is because the near-field modulation and wavefront distortion are more serious in the walk-off direction than those in the perpendicular direction.

In conclusion, we simulate the impact of wavefront phase distortions of pump on the beam quality of signal by using a numerical model of OPA. Numerical results show that, if the walk-off directions of the pump and idler waves are not identical, the walk-off effect is the main factor leading to degradation of the beam quality of the signal as OPA runs in unsaturation regime. When OPA runs in supersaturation regime, the center-sunken spatial beam shapes induced by deep saturation of OPA plays a dominant role in the degradation of beam quality. We can also draw the conclusion that the unidentical walk-off directions of the pump and idler waves, which cause the spatial relative displacement of the wavefront phases between the pump and idler waves, are the main factors leading to the transfer of phase distortions of the pump beam to the signal. So, when the wavefront phase of the pump is distorted seriously, in order to maintain the beam quality of OPA, we should reduce the angle between the walk-off direction of pump and the direction of idler and thus reduce the transfer of phase distortion of the pump beam to the signal by optimizing the noncollinear angle in OPA appropriately.

This work was supported by the National "863" Program of China under Grant No. 2007AA804801.

References

1. I. N. Ross, P. Matousek, M. Towrie, A. J. Langley, and J. L. Collier, Opt. Commun. **144,** 125 (1997).
2. M. J. Guardalben, J. Keegan, L. J. Waxer, V. Bagnoud, I. A. Begishev, J. Puth, and J. D. Zuegel, Opt. Express **11,** 2511 (2003).
3. I. N. Ross, P. Matousek, G. H. C. New. and K. Osvay, J. Opt. Soc. Am. B **19,** 2945 (2002)
4. I. N. Ross, G. H. C. New, and P. K. Bates, Opt. Commun. **273,** 510 (2007).
5. C. Dorrer, A. V. Okishev, I. A. Begishev, J. D. Zuegel, V. I. Smirnov, and L. B. Glebov, Opt. Lett. **32,** 2378 (2007).
6. Y. Wang, X. Pan, J. Wang, L.Wang, X. Li, and Z. Lin, Acta Opt. Sin. (in Chinese) **29,** 980 (2009).
7. I. Jovanovic, J. R. Schmidt, and C. A. Ebbers, Appl. Phys. Lett. **83,** 4125 (2003).
8. I. Jovanovic, B. J. Comaskey, and D. M. Pennington, J. Appl. Phys. **90,** 4328 (2001).
9. X. Wei, L. Qian, P. Yuan, H. Zhu, and D. Fan, Opt. Express **16,** 8904 (2008).
10. R. A. Baumgartner and R. L. Byer, IEEE J. Quantum Electron. **15,** 432 (1979).

11. D. Eimerl, J. M. Auerbach, and P. W. Milonni. J. Mod. Opt. **42,** 1037 (1995).
12. Y.-H. Wang, X. Pan, X.-C. Li, and Z.-Q Lin, Chin. Phys. Lett. **26,** 024211 (2009).
13. Q. Yang, A. Guo, X. Xie, F. Zhang, M. Sun, Q. Gao, M. Li, and Z. Lin, Chinese J. Lasers (in Chinese) **35,** 1970 (2008).
14. A. E. Siegman, Proc. SPIE **1224,** 2 (1990).
15. A. V. Smith and M. S. Bowers, J. Opt. Soc. Am. B **12,** 49 (1995).
16. A. E. Siegman, G. Nemes, and J. Serna, in *DPSS (Diode Pumped Solid State) Lasers: Applications and Issues*, M. Dowley, edn., OSA Trends in Optics and Photonics (Optical Society of America) **17,** MQ1 (1998).
17. V. Bagnoud, M. J. Guardalben, J. Puth, J. D. Zuegel, T. Mooney, and P. Dumas, Appl. Opt. **44,** 282 (2005).